GEOSCIENCES REVIEW

GeoRev is a free access journal of Bayero University, Kano, Nigeria https://georev.org/index.php/georev

Structural Interpretation of Aeromagnetic Data Over Sheet 103 (Ikara), Northwestern Nigeria Using 3D Euler Deconvolution Technique

[1]Abdulmalik, N. F., [2]Garba, I., [2]Najime, T., [2]Ahmed, I. I

[1]Centre for Energy Research and Training, Ahmadu Bello University, Zaria

[2]Department of Geology, Ahmadu Bello University, Zaria

ARTICLE INFORMATION

PISSN 3141-3021 EISSN 3141-303X

Article history:
Received 21 February 2026
Revised 17 May 2026
Accepted 9 June 2026
Available online 29 July 2026

Keywords:
Deconvolution
Equator
Derivative
Structures
Euler

https://doi.org/10.70882/georev2026.2(1)16

ABSTRACT

The Nigerian Basement Complex is characterized by numerous extensive fractures, most of which are concealed beneath the surface. This research aims to identify and delineate these fractures within the north-central part of the basement complex and elucidate their tectonic evolutionary occurrence. To achieve this, High-Resolution Aeromagnetic Data (HRAD) of Sheet 103 (Ikara) were acquired and processed using Reduced-to-Equator (RTE), First Vertical Derivative (FVD), Analytic Signal, and 3D Euler Deconvolution techniques. These were used to interpret the characteristics of anomalous bodies and delineate regional fractures across the fracture and shear zones. The results revealed very low magnetic signatures of an anomalous region suspected to be a depression/trough sited between two prominent fractures trending NW-SW. These fractures exhibit moderate to high magnetic susceptibility, with depths ranging from 1.5km to above 2km. Results also reveal a curvilinear/semi-circular magnetic anomaly suspected to be a ring structure. However, the dominant fractures within the study area, trending WNE-ESE and E-W, exceed 1500 meters. The NW-SE regional fractures, as well as minor NE-SW fractures, evolved during the late-stage Pan-African Orogeny (600 ± 150 Ma). In contrast, the WNW-ESE and E-W trending fractures evolved during the Eburnean (1800± 2500 Ma) and Kibaran Orogeny (1100 ± 200 Ma). The results also reveal that the northern parts of the study area exhibit more fractures than the southern parts.

Peer review under the responsibility of Bayero University, Kano. ©
Corresponding author. E-mail address: nanafatima88@gmail.com (Abdulmalik, N. F. *et al*...)

open access

INTRODUCTION

Regional and subsidiary fractures evolve owing to movements and changes in the Earth's crust. Their depths range from shallow to deep and act as plumbing systems and migratory pathways through which hydrothermal and non-hydrothermal fluids flow (Maltman, 1990; Fornwald, 2017; Galerne et al., 2021; Yin et al., 202). Most of these fractures are hidden in the subsurface and are difficult to detect or identify. Discontinuous quartzite ridges serve as structural indicators of the remaining portions of the sample, most of which are not exposed on the surface. However, geophysical analysis is a useful technique for identifying and studying these hidden and revealed fractures.

Geophysical investigations are used for, but not limited to, reconnaissance survey mapping exercises. It unravels, solves, and provides meaningful interpretations of problems concerning deep crustal studies of both lithologies and geological structures and their geometry hidden in the Earth's subsurface (Nwosu, 2018; Reeves, 2005; Dahuwa et al., 2018; Agboola et al., 2024a; Agboola & Beni, 2024). Geophysical surveys reveal fractures in the earth's interior via gravity, seismic, and magnetic measurements at preferential scales (regional and localized) (Dobrin & Savit, 1988; Reeves, 2005; Aminu et al., 2022; Ibrahim et al., 2023).

Reeves et al. (1997) and Betts et al. (2015) acquired and processed aeromagnetic datasets, thereby revealing and recognizing fractures, faults, and shear zones with strike-slip components. The geometry and tectonic evolution of fractures can also be determined using aeromagnetic and ground magnetic data (Betts et al., 2015). Thus, the lateral extensions of fractures were delineated and characterized based on depth derived from the datasets (Gunn et al., 1997a; Direen et al., 2001; Schetselaar, 2001). However, these aeromagnetic data have limitations in detailing and analyzing regional fractures present in an area of interest (Irvine & Smith, 1990; White et al., 2001; Moreira & Iiha, 2011; Moreira et al., 2012).

In structural geology, fracture depth is an important characteristic. The fractures, whether shallow or deep, facilitate the movement of fluids (mineralisation fluids or water) within the lithosphere. To determine fracture depths from airborne or ground magnetic data, the 3D Euler Deconvolution technique is employed. Three-dimensional (3D) Euler Deconvolution is a powerful tool for determining the geometry, depth, and location of magnetic anomalies caused by multiple and isolated sources in metres (m) or kilometres (km) (El Dawi et al., 2004).

Euler's homogeneity equation is inverted over a data window at each point to accomplish 3D Euler Deconvolution (Thompson, 1982; Reid et al., 1990; Dare & Ayodeji, 2015). Reid et al. (1990) explained the use of 3D Euler Deconvolution as a boundary detector and depth estimator. It is preferred over other techniques because its formula, known as Euler's equation, is independent of geological models and is insensitive to changes in magnetic inclination, declination, or remanence (Whitehead & Musselman, 2008).

The relationship between the anomaly source and its gradient components (x, y, and z) and the magnetic field, with a degree of homogeneity represented by a Structural Index (S.I.), is referred to as "3D Euler Deconvolution". The Structural Index (S.I.), which is defined as the rate of alteration with distance in physical terms, indicates the degree of homogeneity of a source body and the rate at which a source geometry at a certain anomalous field diminishes with distance. 3D Euler Deconvolution uses a Structural Index to produce depth estimates of variations in geological structures (Thompson, 1982). The source geometries of the crusts include rock contacts (at 0.0–0.5 S.I.); dikes and sills (at 1.0- 1.5 S.I.); cylinders and pipes (at 2.0-2.5 S.I.); and spheres (at 3.0- 3.5 S.I.). As stated by Thompson (1982), Reid et al. (1990), Whitehead and Musselman (2008), Osinowo and Olayinka (2013), Kayode et al. (2016b), and others, it can be defined as the field's measured "fall-off" in relation to a given source's distance.

Lawal et al. (2016) and Awoyemi (2017) employed 3D Euler Deconvolution on aeromagnetic data from Ilorin and Osi (north-central Nigeria), as well as the Ilesha area and its surroundings, to identify the depths and widths of various regional cracks. However, previous work carried out on Sheet 103 (Ikara) used FVD and the Analytic Signal to delineate lineaments (Balarabe et al., 2017). It was recommended that, for further tectonic interpretations of this area, a quantitative approach would provide more detail. Hence, the "3D Euler Deconvolution" was efficiently carried out during RTE processing to delineate lineaments, estimate their depths, and determine their orientations. This paper focuses on the application of 3D Euler Deconvolution on the entire Sheet 103 (Ikara) underlain by the basement complex to ascertain, evaluate, and interpret the lineaments generated from the subsurface. The results obtained from the FVD, Analytic Signal, and 3D Euler Deconvolution were correlated to determine the region's conclusive structural/tectonic evolution.

The Nigerian Basement Complex and Regional Faults

One of the largest crustal complexes resulting from the interaction of the active Pharusian continental margin of the Congo Craton with the passive continental margin of West Africa is the Nigerian Basement Complex, which has undergone numerous orogenic episodes (Burke & Dewey, 1972; Dada, 2006). It is situated south of the Tuareg Shield, northwest of the Congo Craton, and east of the West African Craton (Black et al., 1979; LeBlanc, 1981; Caby et al., 1981). The Nigerian Basement Complex lies in the Neoproterozoic Trans-Saharan band, commonly referred to as the Pan-African Belt. The Congo Craton, the West African Craton, and the East African Block collided to form it (McCurry, 1976). Caby (1989) and Boullier (1991) proposed that the Neoproterozoic Trans-Saharan Belt extended from North Africa to Brazil because of several deformational features, including zones of weakness, metamorphism, and the extrusion of alkaline to calc-alkaline volcanics (Wright, 1976; McCurry & Wright, 1977; Holt et al., 1978). It was created by several collisions among sedimentary basins, island arcs, and fragments of continental crust dating to 750–500 million years ago (Ajibade & Wright, 1989; Wright et al., 1985) (Fig. 1).

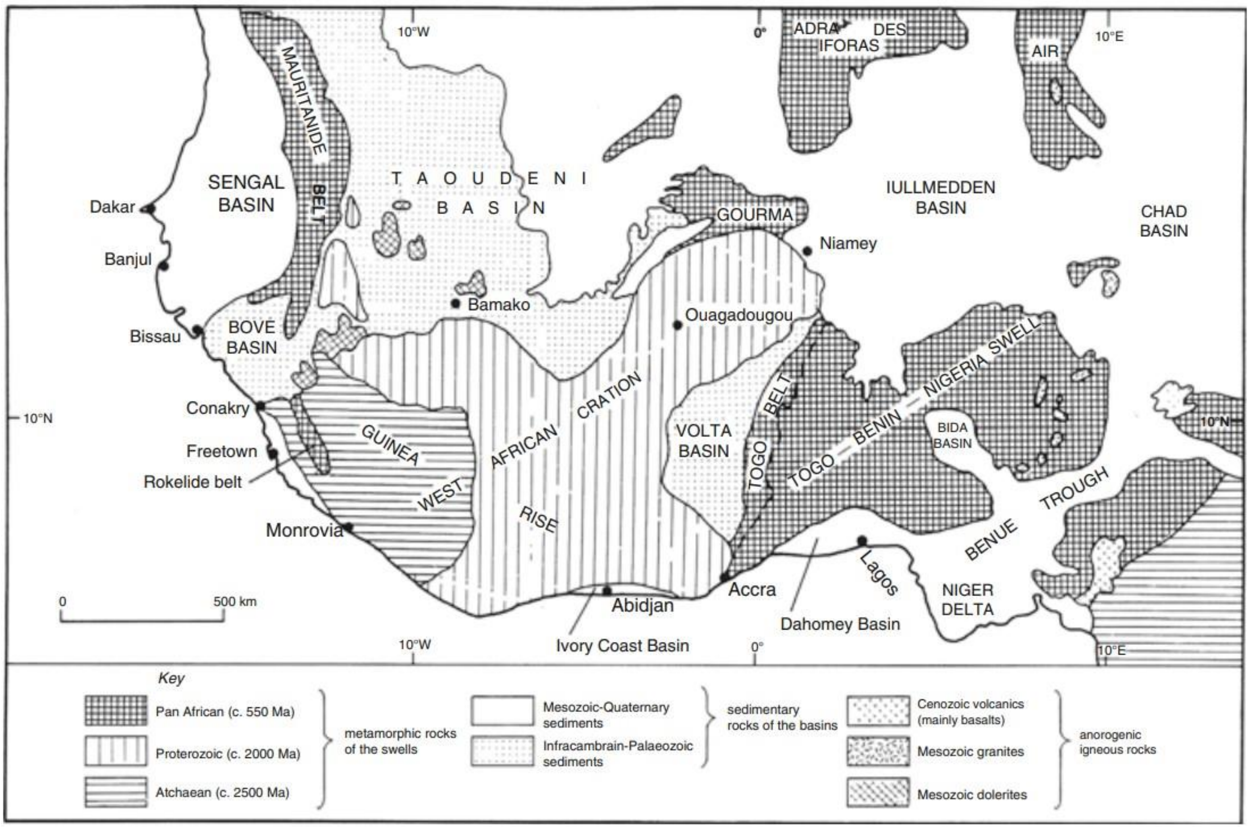

Fig. 1: Generalized geological map of Nigeria in relation to West African geology (adapted from Wright et al., 1985).

There are differences between the Nigerian Basement Complex and the Tuareg Shield. These include the wide-ranging mylonite and shear zones that divide the Tuareg Shield into several structural provinces (Ajibade et al., 1987) (Fig. 2) and the occurrence of higher-grade supracrustal rocks in the Central Hoggar, located in the southern half of the Tuareg Shield. N-S-trending mylonite and fault zones have been identified specifically between the Nigerian Basement Complex, even though their formations are identical (Ajibade et al., 1979; Hubbard, 1975).

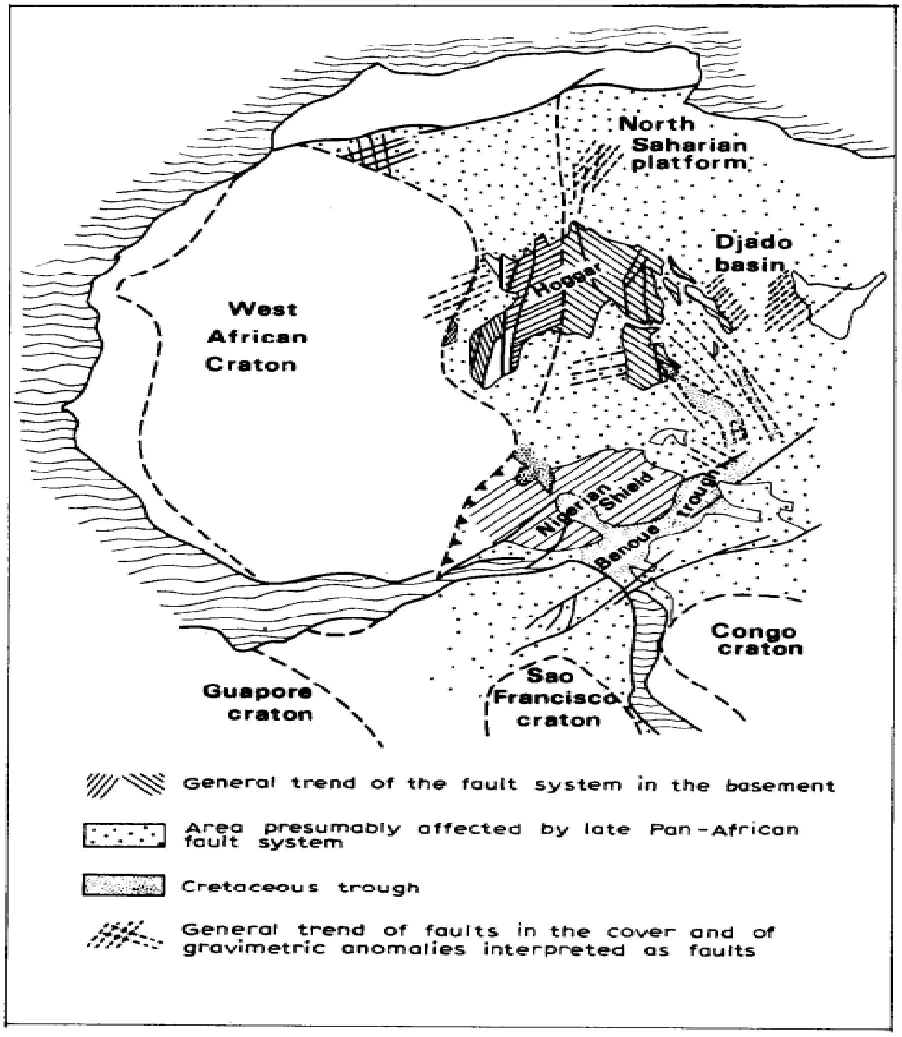

Fig. 2: Geographical scope of the Nigerian and Hoggar (south of the Tuareg) shields' conjugate fault system (derived from Almeida and Black, 1967; in Ball, 1980).

It is thought that at least four major orogenic cycles involved deformation, metamorphism, reactivation, and remobilization, shaping the rocks of the Nigerian Precambrian Basement Complex. Correlations between these cycles have been suggested by the Liberian (2650 ± 150 Ma), Eburnean (1800± 2500 Ma), Kibaran (1100 ± 200 Ma), Pan-African (600 ± 150 Ma), Odeyemi (1981), Rahaman et al. (1983), Grant (1970), Van Breemen et al. (1977), Grant (1978), and others. Based on the International Geologic Time Scale (2002), these ages correspond to the following periods: Mesoproterozoic to Neoproterozoic (1600 to 1000 Ma) for the Kibaran; Paleoarchean to Mesoproterozoic (3600 to 1600 Ma) for the Liberian and Eburnean; and Neoproterozoic to Early Palaeozoic (1000 to 545 Ma) for the Pan-African. Each of these orogenies structurally marks the Basement. Hence, the Nigerian Basement is linked to intricate constructions. However, the most recent and widespread Pan-African orogenic event has largely overprinted the earlier three cycles. This collision established a dominant N-S to north-northeast-southwest structural pattern across the entire Nigerian Basement Complex (Russ, 1957; McCurry, 1973, 1976; Rahaman, 1988; Obaje, 2009). As part of the Pan-African mobile belt, the Nigerian basement consists of older crustal fragments from the Archean, Proterozoic, and Mesozoic periods (Grant, 1970; Grant et al., 1972; Oversby, 1975; Dada, 1998). The collision of these crustal fragments led to the formation of various deformational features, including metamorphism, zones of weakness, and the extrusion of alkaline to calc-alkaline volcanic rocks (Wright, 1976; McCurry & Wright, 1977; Holt et al., 1978). During the Pan-African Orogeny (600±150 Ma), several reactivation episodes occurred within the Nigerian Basement Complex (Burke & Dewey, 1972; Black et al., 1979; LeBlanc, 1981; Caby et al., 1981; Turner, 1983; Fitches et al., 1985; Wright et al., 1985).

According to McCurry (1976) and Rahaman (1976), the Pan-African ultimate tectono-thermal event was so extensive that it obliterated prior buildings. However, some contend that although the Pan-African event was broad in scope, the ruins of older structures in the Basement were not entirely homogenized by it (Grant, 1978; Onyeagocha & Ekwueme, 1982; Ekwueme, 1987; Oluyide, 1988). This latter group agrees that separate structural tendencies emerged from the diverse orogenies. In terms of structure, Rahaman (1976) stated that the Nigerian Basement Complex had two folding stages connected to the Pan-African (600±150 Ma) Older Granite orogeny. He added that a pronounced N-S foliation tendency, the product of prolonged E-W stress, characterizes the Pan-African Orogeny. Significant structural features exhibiting polyphase deformation include foliation, major and minor folds, joints, faults, and lineations. While the E-W and WNW-ESE lines are thought to provide evidence of pre-Pan-African deformation and metamorphism, most likely resulting from the Eburnean/Kibaran orogeny, the NE-SW trends show evidence of penetrative Pan-African deformation.

Study Area

The research area is located in northwest Nigeria, within the North-Central Basement Complex, spanning latitudes 11° 00′ 00′ N to 11° 30′ 00′ N and longitudes 08° 00′ 00′ E to 08° 30′ 00′ E. Covering an area of 3,032 square kilometers, the topography is documented on Sheet 103 (Ikara), a 1:100,000 scale map given by the Department of the Surveyor General of the Federation, Abuja, Nigeria (2008). The Ikara, Tudun Wada, and Kiru Local Government Areas in the states of Kaduna and Kano are responsible for this area. It borders Kiru, Bebeji, and Tudun Wada in Kano State and Makarfi, Soba, and Kubau Local Government Areas in Kaduna State. The primary rock formations in the underlying lithology are gneiss and granite. The general topography of the study area ranges from slightly rugged in the southern parts to mostly moderately undulating terrain in the northern parts. Topography is highest towards the southeast at about 738.4m, then decreases towards the southwest, with heights ranging from about 691.0m to 700.0m. It gently slopes downwards towards the northwest, with elevations ranging from about 569.0m to 682.6m, and is lowest in the northeast, where there is a major river basin with elevations ranging from 486.5m to 526.1m. The drainage pattern of the area ranges from trellis to dendritic, with water channels originating in the north-western and eastern parts flowing downstream towards the river basin in the northeast of the study area. The southwestern drainage flows downstream towards the western part of the area. A few other drainages were observed in the southeastern and northwestern parts of the study area. These rivers are structurally controlled by regional intrusive rock/ridge trending NW-SE across the study area. According to the Köppen–Geiger classification, Ikara experiences a tropical savanna climate. The study area falls within the Sudan Climatic region, which is marked by a short rainy season of about five months. Annual temperature ranges generally lie between 21 °C and 31 °C, although minima may occasionally approach 10 °C and maxima may reach 40 °C. Total annual precipitation averages 761 mm, distributed over approximately 101 days with at least 1 mm of rainfall. The location receives an average of 3,868 sunshine hours per year, while daylight duration varies by season (Udo, 1978; Nomadseason, 2025).

MATERIALS AND METHODS

The Nigeria Geological Survey Agency (NGSA) provided the High-Resolution Aeromagnetic (HRAM) data used in this study (NGSA), with a coordinate system/projection of Universal Transverse Mercator (UTM) and the official geodetic datum for Nigeria of the Arc 1960 datum. Geological features (major and minor lineaments) could be directly detected once the data were processed, allowing for the determination of trends and depths. These structures, represented as magnetic anomalies, were detected and recorded by an airborne magnetometer towed behind an aircraft. The flight elevation (altitude), flight line spacing, flight direction, and tie-line spacing all affected the resolution of the aeromagnetic data. The altitude at which the aircraft was flown (flight height) was 80 m; the flight spacing and direction were 500 m and 150°/330° (NW-SE), respectively; the 60°/240° tie-line spacing was set at 5000 m and ran opposite to the flight line. The gridding type is the minimum-curvature gridding method, and the grid mesh size is 50-100 m, given that the flight spacing is 500 m. The

International Geomagnetic Reference Field (IGRF) served as the basis for the specific correction of aeromagnetic data (2004–2010). The study region has magnetic field strengths ranging from 33103.6 nT to 32919.3 nT. However, 33,000nT was subtracted from all the units (magnetic intensities) recorded to enable smooth running and computation of results in software packages (IGRF:2004-2010).

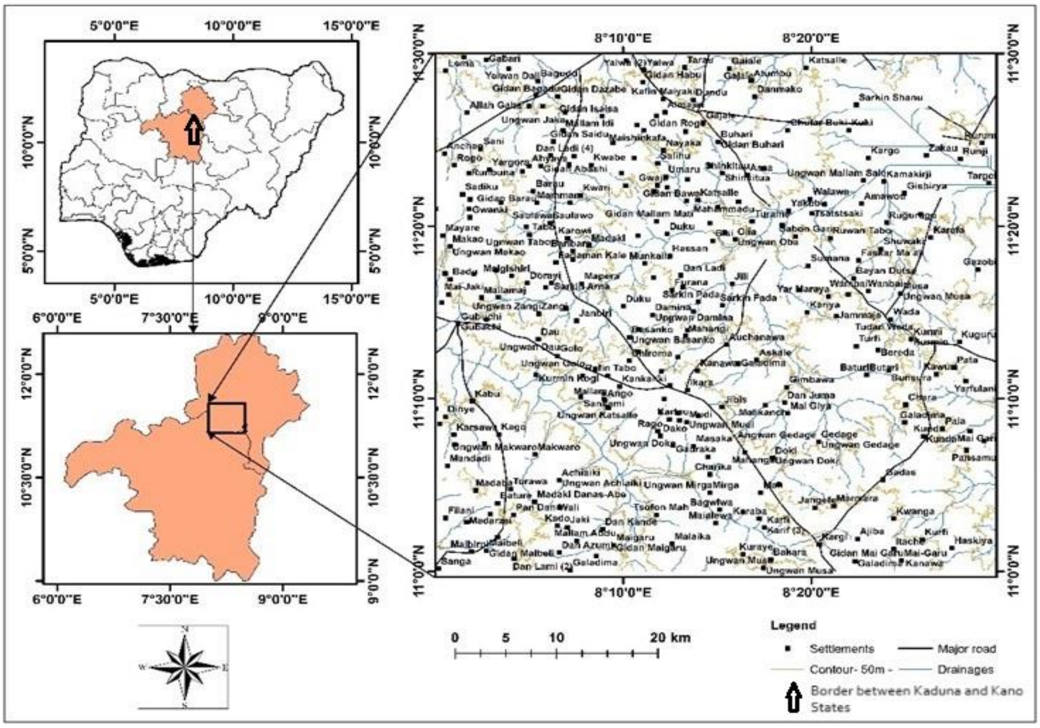

Fig. 3: Map of the study area (right) covering parts of Kaduna and Kano States (bottom left). The arrow shows the border between Kaduna and Kano States.

Magnetic anomalies may be shifted from their sources at non-polar and non-equatorial latitudes (Salawu et al., 2019); as such, TMI data were reduced to the equator (RTE) for gridding. This centers anomalies on their magnetic sources and is equally suitable for low-latitude regions such as the present research area. The RTE filter was preferred on the assumption that the observed magnetic field is due to induced magnetic effects. This assumption is based on the fact that the study area has no mafic or volcanic rocks, as it is dominantly underlain by gneisses and granites (Abdulmalik & Ahmed, 2024). Earth's present-day magnetic field overwhelmingly induces the weak natural magnetization of these rocks. This makes the application of the RTE filter, which corrects for the effects of dipolar-induced magnetism at low latitudes, a fundamentally sound and effective processing step. The parameters for applying the reduction-to-equator filter include inclination (magnetic dip angle is approximately 3.0° north; a positive angle indicates the field vector is pointing downward into the Earth); declination (magnetic declination is approximately -2.9° west; a negative value indicates magnetic north is west of true north); and total magnetic Intensity is approximately 33,120 nT. The anomalies of the resulting TMI-RTE anomaly maps are shifted such that they are centred over their respective sources. Shorter-wavelength anomalies were muted to improve the signal-to-noise ratio and reduce noise in the data. It works best for geological interpretations.

The Analytic Signal and First Vertical Derivative were computed from the RTE grid. The first vertical derivative (FVD) was used to enhance the edges of magnetic anomalies and to enable more distinct imaging of the causative structures. It shows areas with shallow-to-deep anomalies, including lineaments and delineated zones. The enhancement of FVD revealed sharper edges of magnetic anomalies, representing structural features, and provided clearer imaging of causative structures. It revealed structures both closer and farther from the surface, with short and long wavelengths, respectively (Reeves, 2005). Vertical derivative, which is also named vertical gradient||) Filters preferentially amplify short-wavelength components of the field at the expense of longer wavelengths (Foss, 2011). Vertical derivative filters (in this case, "first") are generally applied to gridded data using FFT (Fast Fourier Transform) filters. Various vertical derivatives of the magnetic field can be computed by multiplying the amplitude spectra of the field by a factor of the form

$$1/n\ [(u^2+v^2)1/2]^n$$

Where n is the order of the vertical derivative/gradient, this vertical derivative is physically equivalent to measuring the magnetic field concurrently at two points vertically overhead each other, subtracting the data, and dividing the result by the vertical spatial separation of the measurement points (Okpoli, 2019). The Analytic Signal (A. Signal) is a filtering technique used to delineate structures and lithologies from magnetic susceptibility data. It is used for boundary detection, which prominently reveals magnetic anomalies (Balarabe et al., 2017; Lawal, 2020). The first researcher to use this concept was Nabighian (1972), who applied it to interpret aeromagnetic data and to detect structures responsible for observed magnetic anomalies in a given area. These constitute the qualitative interpretation aspect of the results. He used it to interpret aeromagnetic data, to detect the structures responsible for the observed magnetic anomalies across an area, to enhance magnetite-rich or magnetite-depleted zones distinguishable from host rocks, and to detect the edges of magnetic anomalies/bodies with the expression below:

$$AS(x,y)=\sqrt{\left(\frac{\partial t}{\partial x}\right)2+\left(\frac{\partial t}{\partial y}\right)2+\left(\frac{\partial t}{\partial z}\right)2}$$

Whereby the first derivatives $\partial T/\partial x$; $\partial T/\partial y$; $\partial T/\partial z$ of the magnetic field are in the x, y, and z directions of differentiation.

To estimate fracture depths throughout the study area, 3D Euler Deconvolution was employed, followed by a tolerance-based solution-reduction process to generate a 3D Euler map of clustered solutions. 3D Euler Deconvolution is achieved by flipping the homogeneity equation of Euler over a certain amount of data at each location (Thompson, 1982; Reid et al., 1990; Dare & Ayodeji, 2015). For each grid point within a window, a collection of techniques is applied to solve Euler's equation (Whitehead & Musselman, 2008). Geophysical maps were processed using the 3D Euler Deconvolution technique, which revealed the positions and depths of geologic structures associated with magnetic anomalies in the 2D grid. In contrast, the solution to Euler's homogeneity equation below served as the foundation for the typical 3D Euler Deconvolution:

$$(x - x_0)\ \partial T/\partial x + (y - y_0)\ \partial T/\partial y + (z - z_0)\ \partial T/\partial z = N\ (B - T)$$

where the derivatives of the field in the x, y, and z directions are $\partial T/\partial x$, $\partial T/\partial y$, and $\partial T/\partial z$. Where the causal magnetic source's point (x0, y0, z0) is where the total field T is measured (x, y, z), for the full field, "B" represents the overall value. It connects the position of the sources to the magnetic or gravitational field and its constituents by a degree of uniformity "N" that can be interpreted as a Structural Index, according to Thompson (1982), Mushayandebvu et al. (2001), Nabighian and Hansen (2001), and Fitzgerald et al. (2003). This is the original version of Euler's equation before it was extended by other scholars (see equation above).

$$(x - x_0)\ \partial T/\partial x + (y - y_0)\ \partial T/\partial y + (z - z_0)\ \partial T/\partial z = A$$

In this case, A combines the features of amplitude, strike, and dip, which are difficult to distinguish clearly (Reid et al., 1990). 3D Euler Deconvolution will be used for quantitative interpretation of the data, rather than FVD or Analytic Signals.

RESULTS AND DISCUSSIONS

The study area lies within the eastern province of the north-central basement complex, which is occupied by a variety of gneisses and a large volume of Pan-African granitoids (granitic intrusions). Based on field studies and previous work, the study area consists of migmatitic and granitic gneisses, with the former dominant in the northern part and the latter in the southern part. The study area is dominantly made up of varieties of gneisses (migmatitic gneiss, granite gneiss, porphyroblastic gneiss) and older metasediments belonging to the Migmatite-

Gneiss Complex, and the porphyritic granites and medium to coarse-grained granites belonging to the Older Granites (Fig. 4)

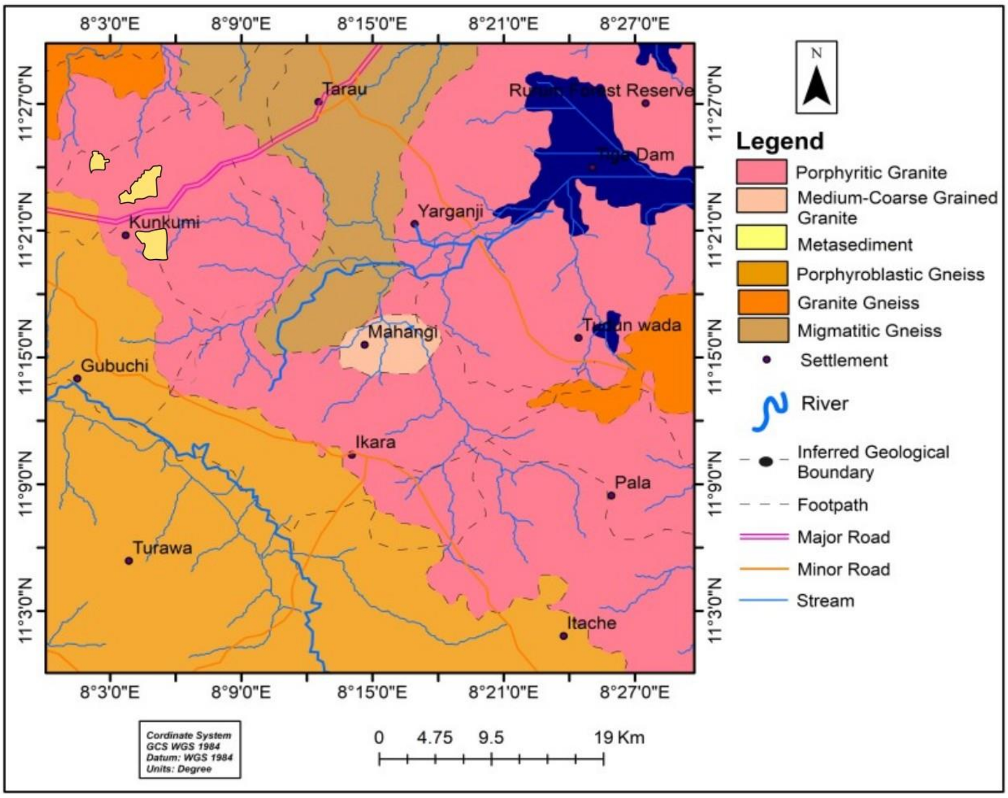

Fig. 4: Geological map of the study area showing the lithological units

Oasis Montaj™ 8.3.3 was used to process the Total Magnetic Intensity (TMI) data and perform the Reduction-to-Equator (RTE). The raw TMI magnetic field strengths (Fig. 5) in the study area range from 33103.6 to 32919.3 nT. The gridded aeromagnetic data for the study area was subsequently processed into RTE and interpreted. The study area is close to the magnetic equator; as such, the magnetic bodies tend to exhibit more frequent low-negative anomalies than high-positive ones. However, the TMI map shows variations in the magnetization field of the magnetic bodies buried underground. It depicts prominent high-amplitude anomalies in extensive, circular, and sub-circular forms distributed across the northern and southern parts of the study area.

RTE pseudo-colour map (Fig. 6) shows various colorations depicting positive and negative magnetic sources of varying wavelengths and amplitudes ranging from (-83.9nT to 81.1nT). RTE centered the magnetic anomalies on their sources to aid interpretation. As such, the visual description of the map segregates the study area into 2 major domains: the first domain, which is characterized by medium to low negative magnetic anomalies (-83.9nT to -1.1nT), is observed at the northeastern area from Rurum Forest Reserve, Tiga Dam, towards a few areas around Kunkumi, heading down south of Gubuchi, areas north of Ikara, Mahangi, and the southeast corner of the study area around Itache. These anomalies trends mainly WNW-ESE, E-W, and NW-SE, with a few trending NE-SW. These areas are underlain by mainly porphyroblastic, migmatitic and granite gneisses which evolved during the pre-Pan-African Orogeny (Grant et al.,1972; Oversby, 1975; Ogezi, 1977; Dada, 1989; Bruguier et al., 1994); the second domain comprises of high positive magnetic anomalies (1.0nT to 81.1nT), observed mainly in parts of the north east and extends down towards the southeast (areas around Tudun Wada and Pala), and from areas extending from the northwestern corner of the study area (west of Tarau) to the east (Gubuchi). These anomalies are predominantly oriented NW-SE and NE-SW, with a few trending E-W. These anomalies are primarily exhibited by porphyritic granites that formed during the Pan-African Orogeny (Van Breeman et al., 1977; Rahaman et al., 1983; Rahaman, 1988; Ademeso & Alaba, 2007).

The First Vertical Derivative (Fig 7) was processed from the RTE and revealed numerous linear and curvilinear fractures that extend from tens to hundreds of kilometres and trend as follows: WNW-ESE, NNW-SSE, NW-SE, NNE-SSW, NE-SW, N-S, and E-W. Two major regional/extensive fractures trending NW-SE were observed to crosscut the study area. The E-W and WNW-ESE were suggested to have evolved from Eburnean (1800± 2500 Ma) to Kibaran (1100 ± 200 Ma) Orogeny (Rahaman, 1976, 1988; Dada, 1989), and the NE-SW and NW-SE fractures evolved during the late Pan-African (600±150 Ma) (Grant, 1970; Turner & Webb, 1974; Burke et al., 1976).

The Analytic Signal (Fig. 8) is a filtering process applied to the RTE that reveals the magnetic susceptibility of these anomalies; the lowest is less than 0.01 × 10^-7 S.I. unit, and the highest is above 0.24 × 10^-3 S.I. unit. The magnetic susceptibility depends on the presence or absence of magnetic minerals in the lithological units. The Analytic Signal revealed magnetic intensities/signatures of the magnetic bodies within the subsurface of the study area, and exhibits extensive, discontinuous, linear, and curvilinear fracture/sheared zones. These anomalous bodies within the study area have very high magnetic intensities. These bodies are quite conspicuous and easy to delineate. The high, moderate, and low magnetic intensities of these bodies exhibit anomalous textural contrasts across the study area. These zones represent variations in the magnetic gradients.

The 3D Euler Deconvolution was used to determine the estimated depths of causative magnetic anomalous bodies or structures across the study area. It was used to determine the location and depth of magnetic bodies and to detect anomalies caused by multiple and isolated sources. The 3D Euler Deconvolution relates the magnetic field and its gradient components (x, y, z) to the anomaly source with a degree of homogeneity expressed as Structural Index (S.I.), hence the name "3D Euler Deconvolution". Structural Index is a measured "fall-off" of the field with distance from the source. Thus, Oasis Montaj™ 8.3.3 was used to estimate the depths of magnetic bodies within the study area using windowed Euler depth solutions. This technique has proven to be a powerful tool for directly determining the depths of causative magnetic bodies (Muzala et al., 1999; Roy et al., 2000). The windowed Euler depth solutions use colour-coded circles; the colours indicate depth ranges, and their sizes represent depth variation within those ranges across the fracture zones (Fig. 9).

Several steps were taken to achieve a clean result of Euler's Deconvolution: grid processing; creation of a solution database; creation of a new map; drawing a base map; plotting solution symbols; solution reduction of the outcome; and plotting. The Euler solutions were superimposed onto the generated FVD and Analytic Signal results (Figs 10 and 11). The 3D Euler cluster solutions from the processed RTE were treated using a windowing technique to minimize uncertainty to the lowest possible level (15%). Tolerance levels were used alongside windowing to reduce this uncertainty and improve edge smoothness. Statistical values for maximum, minimum, and mean solutions, along with Tolerance and Window size values of clusters for S.I 0 and 1 (contacts (0) and dykes (1)) were calculated. Window sizes of solutions could not exceed 20 due to the logarithms, but the tolerance level for the solutions of dykes could exceed 20. Any value above 20 will not generate a result; hence, 15 was used, with a tolerance level of 20 to ensure a higher-quality dataset for interpretation. Hence, the window size and Tolerance levels were varied simultaneously until a preferred window size and Tolerance level were found that yielded a clear representation of lineaments and their estimated depths across the study area.

For clear delineation and exhibition of lineaments represented as dykes within the fracture zones, S.I of 1, a tolerance level of 20%, and a window size of 15 grid cells were utilised after several attempts at variations to arrive at accurate and meaningful results/solutions. This data were used to generate the final 3DEuler image using the Oasis Montaj Software. This gave the estimated depths of the fractures within the basement rocks underlying the study area. The higher the tolerance, the greater the noise from shorter wavelengths at shallow depths; as such, shorter wavelengths from the surface had to be eliminated by decreasing the tolerance level. However, the higher the tolerance level, the higher the cluster solutions; thus, a balance between reducing noise and achieving more accurate solutions had to be found.

The entire study area consists of various fracture and shear zones. As such, the 3D Deconvolution results reveal the estimated depths of these zones basically in three categories: the zones with depths of about >1500m to ≥2000m (within the migmatitic gneisses); zones with depths between >400m to 1500m (within migmatitic gneiss, granite gneiss, porphyroblastic, and porphyritic granite); and zones with depths of about ≤100 to ≤400m (in all the lithological units). Fractures with depths ranging from 400 to 1500m dominate the northern regions compared with the southern parts of the study area. These fractures are found in migmatitic gneiss, granite gneiss, and porphyritic granites. Over thirty-two thousand solutions were generated, the shallowest depth at which a fracture was identified from the solutions was at less than 100m (83m), and the deepest fracture(s) were identified above 2000m (2156m).

The FVD and Analytic Signal results display the lateral extensions and magnetic susceptibility of the anomalies, respectively, with estimated depths acquired from the 3D Euler Deconvolution. The lineament solutions from the 3D Euler reveal similar orientations to those generated by the FVD. The cluster solutions derived from the 3D Euler Deconvolution were superimposed over the FVD and revealed a merging correlation with the generated lineaments from the FVD. The above-mentioned orientations of the lineaments from the FVD were as observed from the 3D Euler solutions. Both reveal the positioning of the major NW-SE fractures with depths ranging from 400m to above 2000m; fractures in zones suspected to be curvi-linear structure (northeastern part of the study area) and possible trough presence (northcentral of study area in between two extensive fractures) with depths ranging from 100m to about 2000m; and other fractures with depths below 1500m distributed across the study area.

The 3D Euler solution, superimposed on the Analytic Signal, revealed regions with deep-seated fractures ranging from 1500-2000m that have low magnetic susceptibility; regions that have fractures with depths ranging from 400-1500m have moderate to high magnetic susceptibility, and they dominate the northern regions more than the southern parts of the study area. These fractures are found within the gneisses and the granites. High magnetic susceptibility was observed in parts of the northeast, where the Rurum Forest Reserve and the Tiga Dam are located. These regions are underlain by porphyritic granites with curvilinear features. Low magnetic susceptibility was also observed between the two extensive fractures, which are underlain by migmatitic gneiss. As interpreted from the FVD-Euler, this low magnetic susceptibility zone is suspected to be a possible trough or graben caused by a relay fault between two extensive faults or by extensional stress evolving into a releasing bend. This proposal can be correlated with the research and findings of Ajakaiye et al. (1991), which highlighted the magnetic anomalies and characteristics of major fault zones in the Atlantic basins. The depths of these extensive fractures are consistent with the work of Raimi et al. (2014) and Balarabe et al. (2018). The faults extend beyond the study area; accordingly, the maximum, minimum, and average lengths are 70 km, 56 km, and 63 km, respectively.

The gneisses had more fractures, discordant veins, and dykes relative to the granitic rocks. This was because the gneisses are more competent than the granitic rocks. Higher frequencies, smaller displacements, and shorter faults were observed in the gneissic rocks of the study area. In contrast, lower frequencies, larger displacements, and longer faults were observed in the granitic rocks. This is similar to the analysed and documented works on gneiss and granite rock units by Higgins (1971) and Ball (1980). Tensile fractures (joints) are caused by extensional stress, where no displacement occurs. They are usually oriented parallel to maximum stress (σ_1) and perpendicular to minimum stress (σ_3), and these cracks/fissile structures open horizontally while extending vertically. Metamorphic rocks are stiffer, denser, and drier and therefore tend to exhibit more tensile fractures, whether open or closed, than granitic rocks (Ball, 1980). The fractures that facilitated the formation of discordant structures were older than those that eventually cut across them and evolved into fault planes along which the dissected veins/dykes slid laterally. Based on the ages of these fractures, as determined by geochronological studies, it is logical to conclude that the tectonic evolution of the Pan-African Orogeny superimposed the Eburnean and Kibaran Orogeny fractures. Fig. 12 is the lineament map, which was automatically generated from the FVD-RTE using ArcGIS Software, showing the distributions of the fractures across the fracture/shear zones; and Fig. 13 is the rose diagram (with intervals of 50) that displays the orientations of dominant and least fractures across the study area.

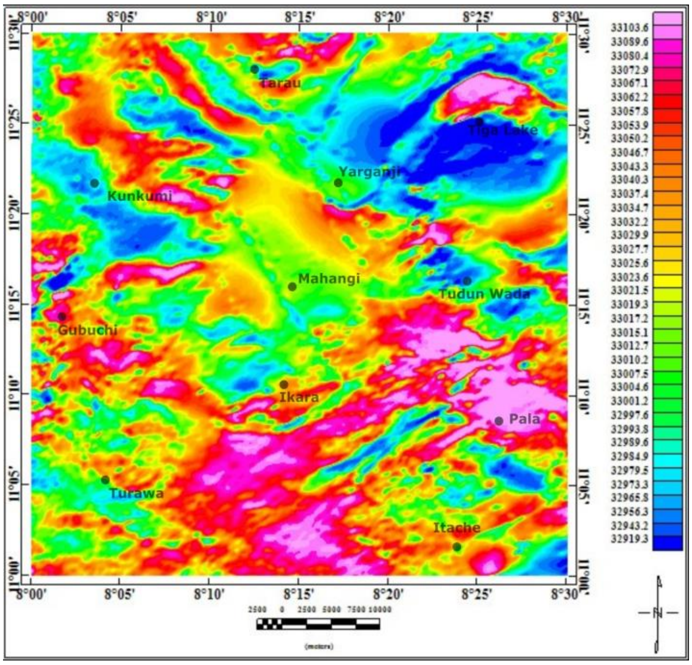

Fig. 5: Total Magnetic Field Intensity (TMI) aeromagnetic data showing regions of high (pink/purple to red) to low (green and blue) magnetic intensities representing structural features and lithological units.

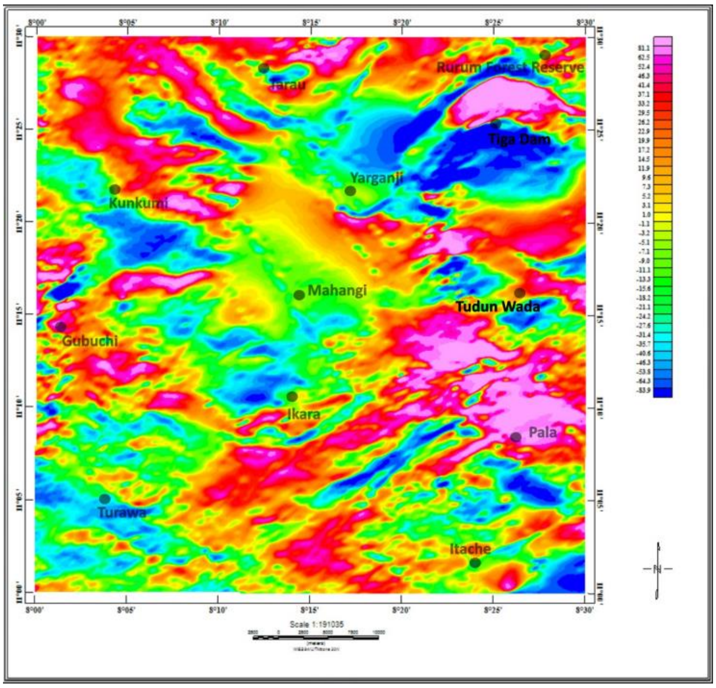

Fig. 6: Reduced-to-equator (RTE) aeromagnetic anomaly map of Sheet 103 (Ikara), processed from the Total Magnetic Intensity grid.

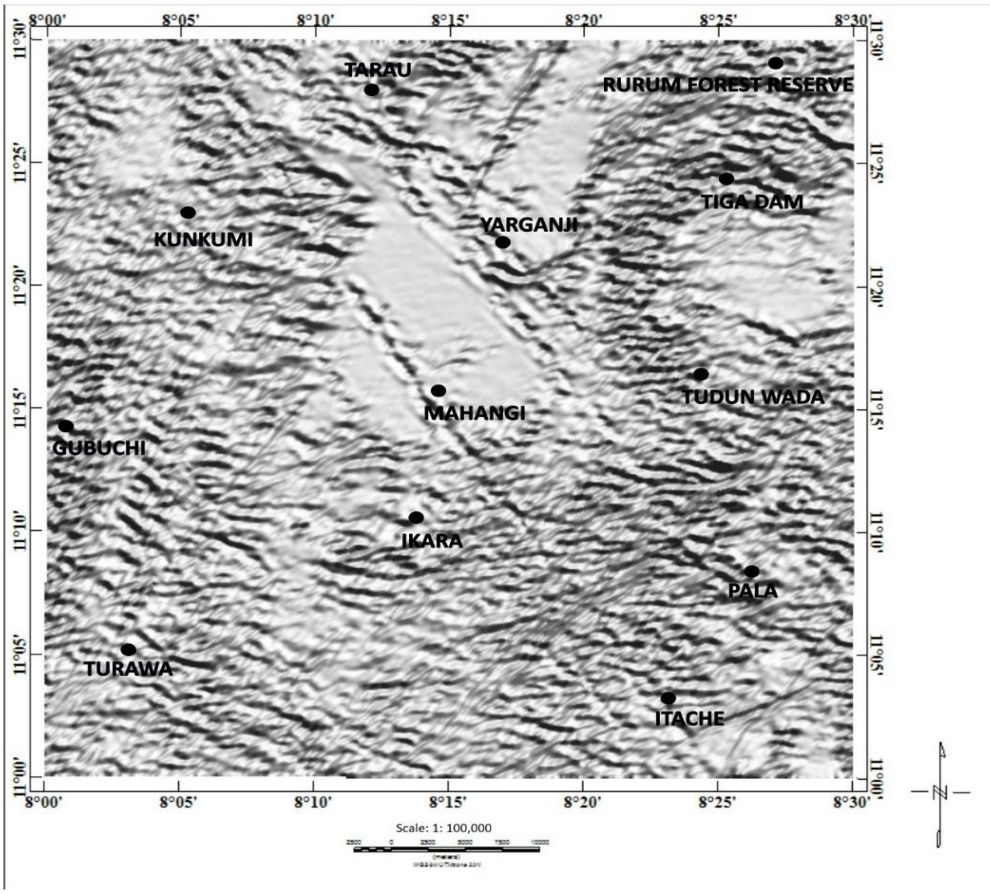

Fig. 7: First Vertical Derivative (FVD) generated from the RTE grid showing regional NW-SE extensive fractures and NE-SW lineaments cross-cutting WNW-ESE and E-W fractures.

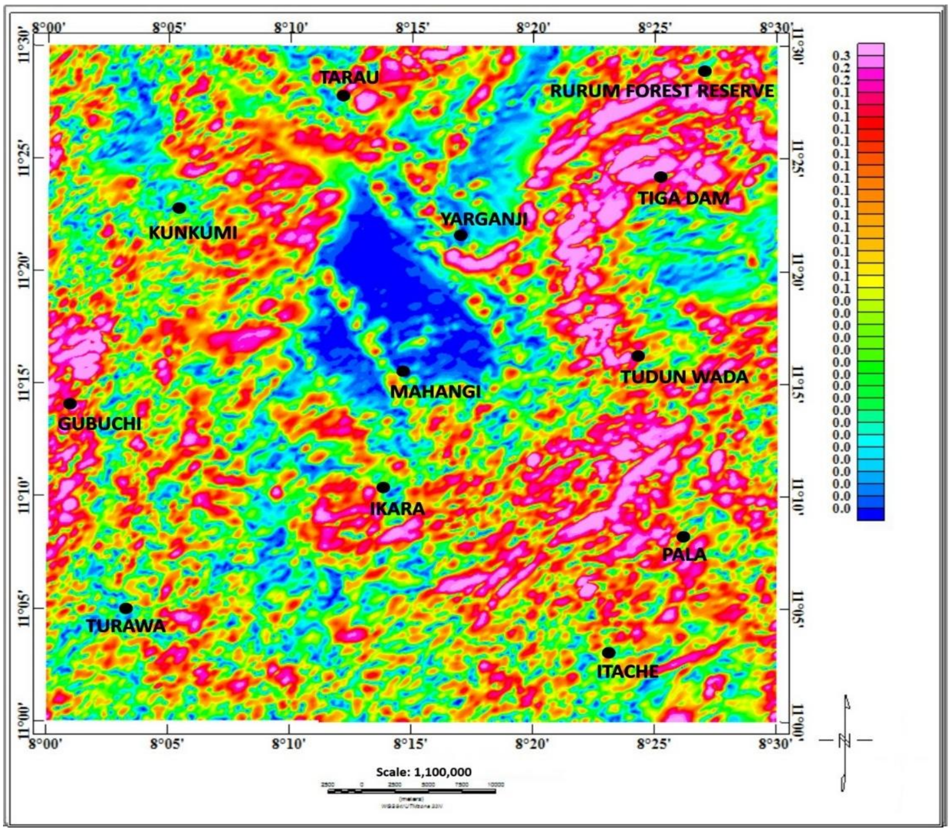

Fig. 8: Analytic Signal produced from the RTE grid, revealing low-to-high magnetic anomalies of extensive structural features within the fracture and sheared zones identified within the subsurface.

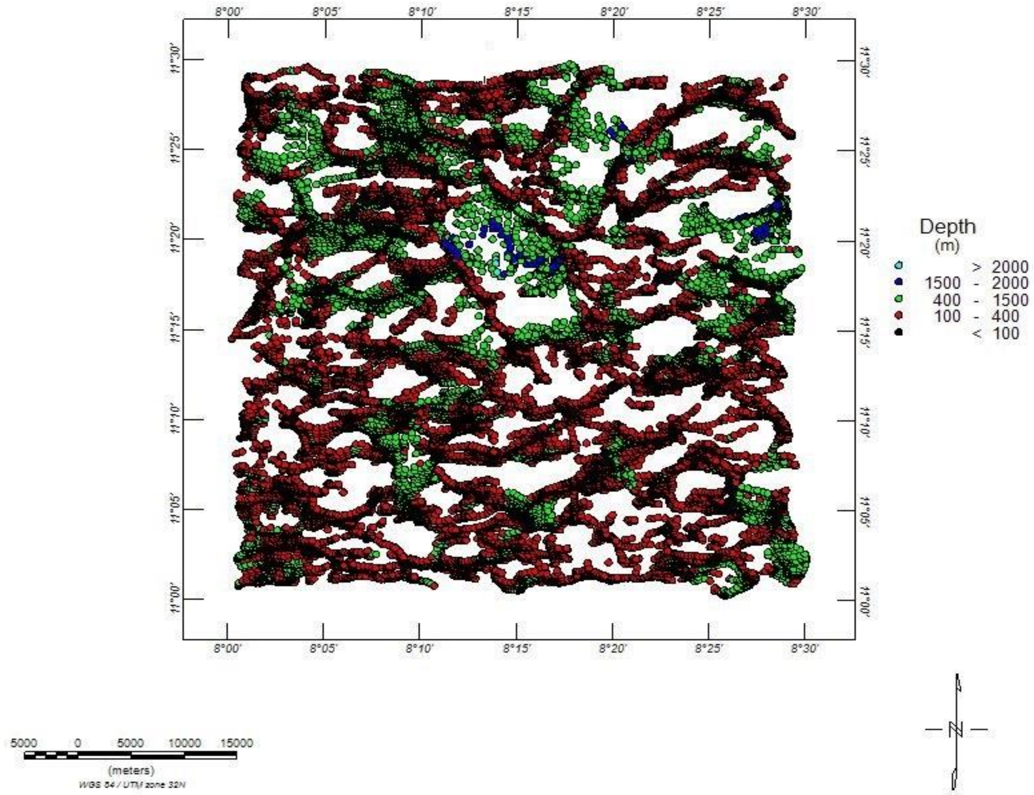

Fig. 9: 3D-Euler Deconvolution solution clusters showing estimated depths of regional fractures ranging from less than 100m to above 2000m.

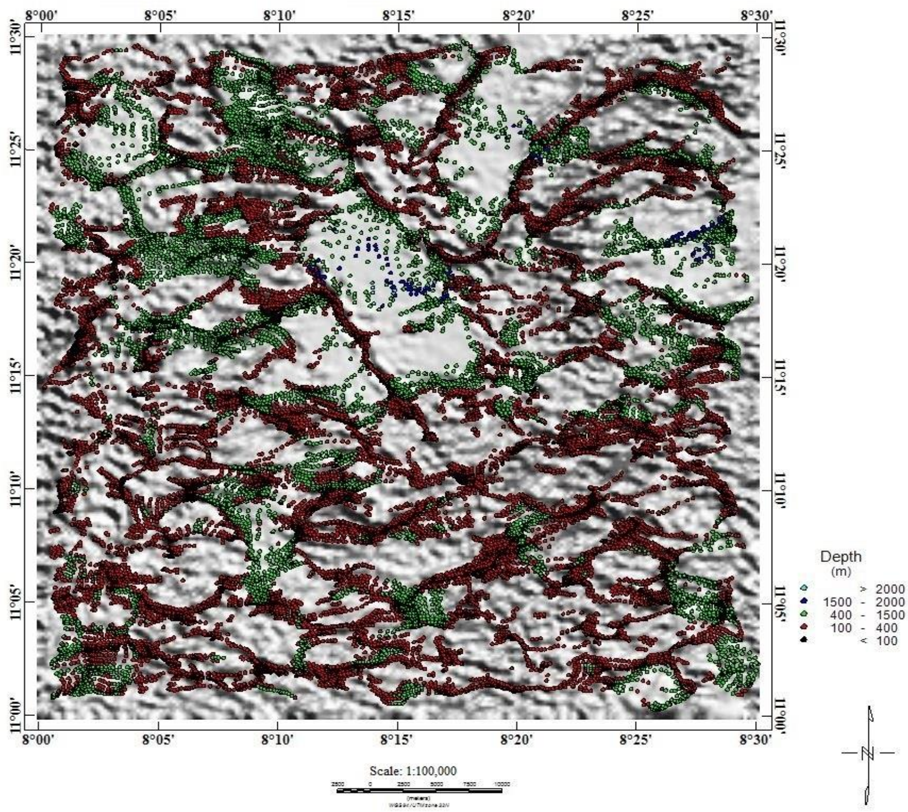

Fig. 10: 3D Euler Deconvolution cluster solutions superimposed on FVD-RTE. This shows a close correlation between the solutions generated from Euler and the fractures from the FVD.

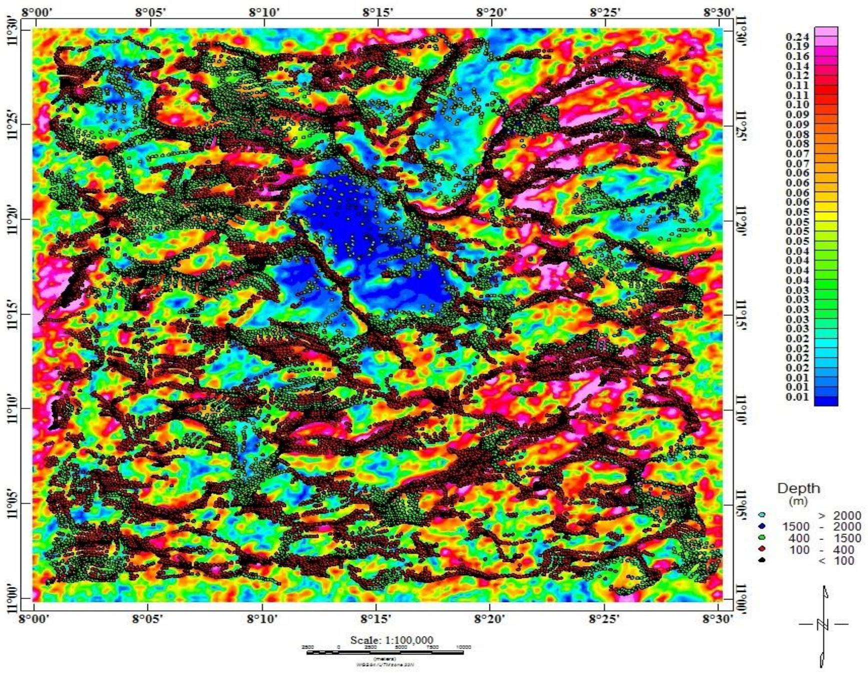

Fig. 11: 3D Euler Deconvolution solutions superimposed on the Analytic Signal-RTE. This shows the magnetic susceptibilities of the anomalous bodies and fractures, along with their corresponding depths.

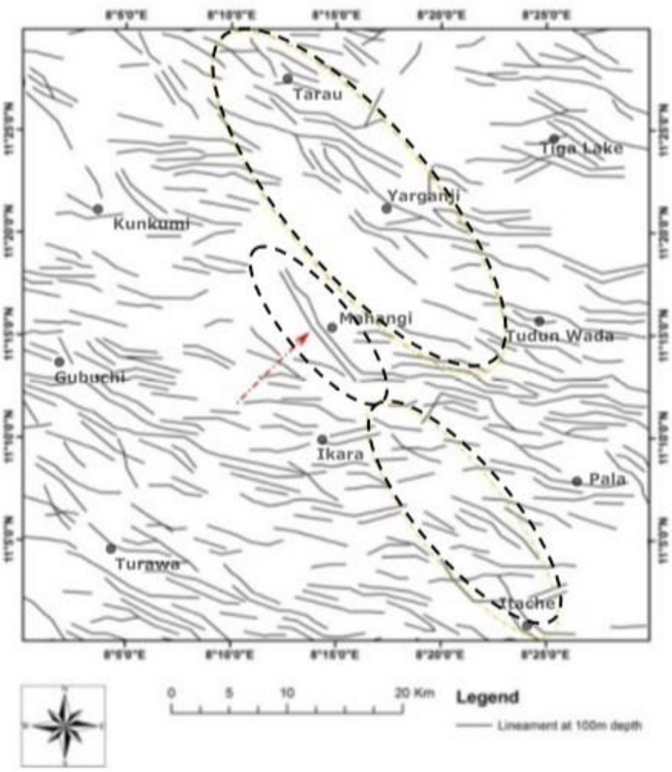

Fig. 12: Lineament map generated from FVD: the arrows and broken lines show minor and major fractures trending NE-SW and NW-SE, which are superimposed on the WNW-ESE and E-W fractures.

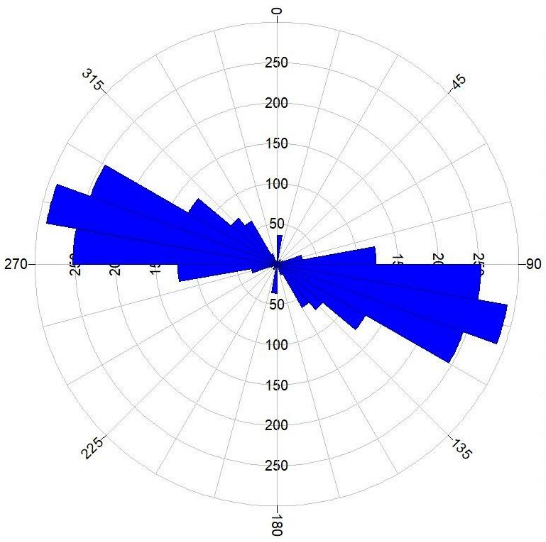

Fig. 13: Rose plot showing WNW-ESE and E-W lineaments to be dominant and NW-SE, NE-SW, and N-S lineaments to be least dominant.

CONCLUSIONS

Qualitative and quantitative geophysical approaches were successfully employed to delineate extensive lineaments, determine their depths and magnetic susceptibilities, and elucidate the tectonic evolution of Sheet 103 (Ikara). This was achieved by processing a Reduced-to-Equator (RTE) from the raw Total Magnetic Intensity (TMI) data. This was further processed to acquire the FVD-RTE and Analytic Signal-RTE and to generate the 3D Euler Deconvolution solutions. RTE revealed magnetic anomalies categorised into two major structural domains with low (negative) and high (positive) magnetic signatures. First Vertical Derivative showed the positions and orientations of linear and curvilinear fractures. The trends of these fractures were predominantly WNW-ESE and E-W, with minor NE-SW, NW-SE, and N-S. Analytic Signal revealed the magnetic susceptibility of the magnetic anomalies (lithological units and structures) across the study area, their proximity to the surface, and the presence of a broad curvilinear magnetic anomaly. The 3D Euler Deconvolution displayed estimated depths of these anomalies (lineaments) in the subsurface. The lineament solutions from the 3D Euler reveal similar orientations of the lineaments as those generated from the FVD. The 3D-Euler Deconvolution solutions revealed the presence and estimated depths along the regional NW-SE fractures, curvilinear structure (circular magnetic anomaly), and other fractures within the fracture/shear zones in the study area. Superimposing the 3D-Euler Deconvolution solutions over the FVD and the Analytic Signal results revealed a clearer understanding and correlation among lineaments, depths, and magnetic susceptibility in the study area. The presence and depth of these fractures will serve as potential migration pathways for fluids (groundwater and mineralisation fluids) within the study area. The results from these two geophysical approaches revealed lineaments with different orientations, suggesting they may have evolved during different Orogenic events. These fractures may lead to further mechanical deformation within the lithologies and serve as migration pathways for hydrothermal fluids and water in Ikara and its environs.

ACKNOWLEDGEMENT

I express my gratitude to the NGSA for their assistance in providing the aeromagnetic data that were used in this investigation.

CONFLICT OF INTEREST

The authors declare that they have no competing interests.

REFERENCES

Abdulmalik, N. F. & Ahmed, I. I. (2024). Lithological and Structural Mapping of Basement Rock Units in the Ikara North-Central Basement Complex, Nigeria. Umaru Musa Yar'Adua University (UMYU Scientifica), Vol. 3, No. 4, Pp. 187-217

Ademeso, O. M. & Alaba, O. A. (2007). Petrography, Geochemistry and Petrogenesis of Some Granitoids in the

Basement Complex around Ondo Area, SW Nigeria. Journal of Mining and Geology, 43(2), 99–110.

Agboola, G., Beni, L. H., Elbayoumi, T. & Thompson, G. (2024a). Optimizing landslide susceptibility mapping using machine learning and geospatial techniques. Ecological Informatics, 81, 102583. https://doi.org/10.1016/j.ecoinf.2024.102583

Agboola, G. & Beni, L. H. (2024). Geospatial Insights: Unraveling Howard Landslide Susceptibility. IGARSS 2024 - 2024 IEEE International Geoscience and Remote Sensing Symposium, 3014–3017. https://doi.org/10.1109/IGARSS53475.2024.10641633

Ajakiaye, D. E., Hall, D.H., Ashiekaa, J.A., & Udensi, E.E. (1991). Magnetic anomalies in the Nigerian continental mass based on aeromagnetic surveys. Tectonophysics, vol. 192, pp. 211–230.

Ajibade, A.C. & Wright, J.B. (1989). The Togo-Benin-Nigeria shield: evidence of crustal aggregation in the Pan-African belt. Tectonophysics: **165**, pp. 125–129.

Ajibade, A.C., Fitches, W.R. & Wright, J.B. (1979). The Zungeru mylonites, Nigeria: recognition of a major tectonic unit. REVUE DE GÉOLOGIE DYNAMIQUE ET DE GÉOGRAPHIE PHYSIQUE, vol. 21: pp. 359–363.

Ajibade, A.C., Woakes, M. & Rahaman, M.A. (1987). Proterozoic crustal development in the Pan-African regime of Nigeria. In: A. Kröner (Editor), Proterozoic Crustal Evolution. Geodynamic Series, American Geophysical Union, vol. 17: pp. 259–271.

Almeida, F.F.M. & Black, R. (1967). Symposium on continental rift. Montevideo Geological comparison of the North-Eastern South America drift and Western Africa. An. Acad. Brasil. Cienc. (Suppl.), pp. 319–377.

Aminu, M. B., Nanfa, C. A., Hassan, J. I., Yahuza, I., Christopher, S. D., & Aigbadon, G. O. (2022). Application of Electrical Resistivity for Evaluation of Groundwater Occurrence Within Adankolo Campus and Environs, Lokoja, North Central, Nigeria. European Journal of Environment and Earth Sciences, 3(1), 14–22. https://doi.org/10.24018/ejgeo.2022.3.1.235.

Awoyemi, M. O., Hammed, S. and Falade, M. Y. (2017). Geophysical investigation of the possible extension of the Ifewara fault zone beyond the Ilesa area, southwestern Nigeria. Arab Journal of Geoscience, vol. 10(2): page 27. https://doi.org/10. 1007/s12517-016-2813-z

Balarabe, B., Lawal, K. M., Ahmed, A. L., Umar, M., Mohammed, M. A., & Adamu, A. (2017). The use of Analytic Signal and First Derivative techniques to gain insight into aeromagnetic anomaly patterns in part of Ikara, Nigeria. FUW Trends in Science and Technology Journal, Vol. 2 No. 2 pp. 684 – 690.

Balarabe, B., Bagudu, L., Umar, M., and Mustapha. S. (2018). Application of Euler and Werner Deconvolution techniques for the interpretation of aeromagnetic data around the Banke Ring Complex, Nigeria. FUW Trends in Science & Technology Journal. 2018: Vol. 3 No. 2A, pp. 501 – 506.

Ball, E. (1980). An example of very consistent brittle deformation over a wide intracontinental area: The Late Pan-African fracture system of the Taureg and Nigerian shield. Tectonophysics: 16: 363–379.

Black, R., Ball, E., Bertrand, J.M.L., Boullier, A.M., Caby, R., Davison, I., Fabre, J., Leblanc, M. & Wright, L.I. (1979). Outline of the Pan-African geology of Adrar des Iforas (Rep. of Mali). Geologische Rundschau, vol. 68(2): pp. 543–564.

Betts, P. G., Ailleres, L., Armit, R., Blaikie, T., & Jessell, M. (2015). Structural Geophysics. Extended Abstract of the 14th SAGA Biennial Technical Meeting and Exhibition. Pages 1–4.

Boullier, A. M. (1991). The Pan-African Trans-Saharan belt in the Hoggar shield (Algeria, Mali, Niger): a review. In: DALLMEYER, R.D. &LEC'ORC'HE, J.P. (editors) The West African Orogens and Circum-Atlantic Correlatives. Springer-Verlag, Berlin, pp.85–105.

Bruguier, O., Dada, S., Lancelot, J.R. (1994). Early Archean component (3.5 Ga) within a

3.05 Ga orthogneiss from northern Nigeria: U–Pb zircon evidence. Earth and Planetary Science Letters 125, 89–103.

Burke, K. C. & Dewey, J.F. (1972). Orogeny in Africa; In African Geology, edited by Dessauvagie, T.F.J. and Whiteman, A.J. University of Ibadan. Pp. 583–608.

Burke, K., Freeth, S. J. & Grant, N. K. (1976). The structure and sequence of geological events in the Basement Complex of the Ibadan area, Western Nigeria. Precambrian Research, vol. 3: pp. 537—545

Caby, R., Bertrand, J.M.L. & Black, R. (1981). Pan-African ocean closure and continental collision in the Hoggar-Iforas segment, Central Sahara: In Precambrian Plate Tectonics. Kröner, A. (Editor); Elsevier Amsterdam, pp. 407–434.

Caby, R. (1989). Precambrian terranes of Benin-Nigeria and northeast Brazil and the late Proterozoic South Atlantic fit. Geological Society of America Special Paper (**230**), pp. 145–158.

Dada, S.S. (1989). "Évolution de la croûte continentale au Nigeria : U-Pb et traceurs isotopiques Sr, Nd et Pb," Thèse de doctorat, Univ. der Sci. Tech. Lang. Montpelier.

Dada, S. S. (1998). Crust-forming ages and Proterozoic crustal evolution in Nigeria: a reappraisal of current interpretations. Elsevier Precambrian Research, vol. 87, pp. 65–74.

Dada, S.S. (2006). Proterozoic evolution of the Nigeria-Boborema province; In: O. Oshin (Editor). The Basement Complex of Nigeria and its mineral resources: A Tribute to Prof. M. A. O. Rahaman: Akin Jinad and Company. Ibadan. Pp. 29–44.

Dahuwa, D., Umar, W., Sani, M. & Abba, L. (2018). Aeromagnetic data analysis of the Tafawa Balewa area using second vertical derivative and Analytic Signal techniques. IOSR Journal of Applied Geology and Geophysics (IOSR-JAGG).Vol. 6(1), pp. 25–32.

Dare, O. and Ayodeji, J. (2015). Geological and Structural Interpretation of Ado-Ekiti, Southwest, and its Adjoining Areas Using Aeromagnetic Data. Adapted from an extended abstract prepared in conjunction with the oral presentation given at the Pacific Section AAPG, SEG, and SEPM Joint Technical Conference, Oxnard, California, AAPG.

Direen, N. G., Lyons, P., Korsch, & Glen, R. (2001). Integrated geophysical appraisal of crustal architecture in the eastern Lachlan Orogen.Exploration Geophysics, **109**, pp. 136–142.

Dobrin, M. B. & Savit, C. H. (1988). Introduction to Geophysical Prospecting, Fourth Edition. McGraw–Hill, New York, page 867.

Ekwueme, B.N. (1987). Structural orientations and Precambrian deformation episodes of the Uwet area, Oban Massif, SE Nigeria. Precambrian Research. Vol. 34, pp. 269–289.

El Dawi, M.G., Tianyou, L., Hui, S. & Dapeng, L. (2004). Depth estimation of 2-D magnetic anomalous sources by using the Euler Deconvolution method. American Journal of Applied Sciences, vol. (1/3), pp. 209–214.

Fitches, R. W., Ajibade, A. C., Egbuniwe, I. G., Hole, R. W., Wright, J. B. (1985). Late Proterozoic Schist Belts and Plutonism in Northwestern Nigeria: Journal of the Geological Society of London, vol. 142: pp. 319–337.

Fitzgerald, D., Reid, A. & McInerney, P. (2003). New discrimination techniques for Euler Deconvolution, 8th SAGA Biennial Technical Meeting and Exhibition.

Fornwald, C. (2017). Geological Society of America Abstracts with Programs. Vol. 49, No. 5; doi: 10.1130/abs/2017RM-293231

Foss, C. (2011). Magnetic data enhancement and depth estimation. In: Gupta H, ed. Encyclopedia of Earth Sciences Series, pp. 736–746.

Galerne, C. Y., Lizarralde, D., Berndt, C., Neumann, F., Höfig, T. W., Stock, J. M., Peña-Salinas, M. E., Negrete-Aranda, R., & Teske, A. P. (2021). Magma plumbing system and associated hydrothermal vents in the Guaymas Basin - geometry and implications, EGU General Assembly 2021, EGU21-13015, https://doi.org/10.5194/egusphere-egu21-13015

Grant, N. K. (1970). Geochronology of Precambrian basement rocks from Ibadan, southwestern Nigeria. Earth and

Planetary Science Letters. Vol. 10: pp. 29–38.
Grant, N. K., Hickman, M., Burkholder, F. R., & Powell, J. L. (1972). Kibaran metamorphic belt in the Pan-African domain of West Africa, Nature (London), vol. 134: pp. 343–349.
Grant, N.K. (1978). Structural distinction between a metasedimentary cover and an underlying basement in the 600 Ma old Pan-African domain of northwestern Nigeria: Geological Society of America; Bulletin, vol. 89: pp. 50–58.
Gunn. P., Maidment, D., and P.Milligan. (1997). Interpreting aeromagnetic data in areas of limited outcrop. AGSO Journal of Australian Geology and Geophysics, vol. 17(2), pp.175–185.
Higgins, M. (1971). Cataclastic Rocks. Professional paper, USA Geological Survey, page 97.

Holt, R.W., Egbuniwe, I., Fitches, W.R., & Wright, J.B. (1978). The relationship between low-grade metasedimentary belts, calc-alkaline volcanism, and the Pan-African orogeny in northwestern Nigeria: Geologische Rundschau, vol. **67**, pp. 631–646.
Hubbard, F.H. (1975). Precambrian crustal development in western Nigeria: indications from the Iwo region. Geologic Society of America Bulletin, vol. 86: pp. 548–554.
Irvine, R. J. & Smith, M. J. (1990). Geophysical exploration for epithermal deposits. Journal of Geochemical Exploration, vol. **36**, pp. 375–412.
Ibrahim, A., Mu'awiya, B. A. & Okechukwu, A. K. (2023). Frequency-Domain Electromagnetic and VLF Data with An Application to Modeling of Basement Structures: A Case Study Within the Ibadan Area, Southwestern Nigeria. International Journal of Research and Innovation in Applied Science, VIII(VI), 156–175. https://doi.org/10.51584/IJRIAS.2023.8616
Kayode, J. S., Nawawi, M. N. M., & Abdullah, K. (2016b). Structural Analysis of Part of the Nigerian South-Western Basement Complex using Aeromagnetic Data. The 7th International Conference on Applied Geophysics and Geophysics towards Sustainable Development of Thailand and AEC.
Lawal, T. O., Salawu, N. B., Orosun, M. M., Ekpumoh, J. I., & Nwankwo, L. I. (2016). Application of the 3-D Euler Deconvolution technique to aeromagnetic data of Ilorin and Osi, North Central Nigeria. Zimbabwe Sci Technol, vol. 11: pp. 66–75
Lawal, T. O. (2020). Integrated aeromagnetic and aeroradiometric data for delineating lithologies, structures, and hydrothermal alteration zones in part of southwestern Nigeria. Arabian Journal of Geosciences, vol. 13: 775, pp. 1-19
Leblanc, M. (1981). The Late Proterozoic Ophiolites of BouAzzer (Morocco) evidence for Pan-African plate tectonics: In Precambrian Plate Tectonics. Kroner, A. (Editor): Elsevier, Amsterdam. P. 435–451.
Maltman, A. (1990). Geological Maps – An Introduction. John Wiley & Sons Ltd, Baffins Lane, Chichester, West Sussex, England, 184 p.
McCurry, P. (1973). The geology of Sheet 21, Zaria, Nigeria: Overseas Geology and Mining Resources, 45.
McCurry, P. (1976). The Geology of the Precambrian Palaeozoic rocks of northern Nigeria- review. In: C.A. Kogbe (Editor), Geology of Nigeria. Elizabethan Publishers and Co., Lagos, pp. 15–39.
McCurry, P. & Wright, J. B. (1977). Geochemistry of calc-alkaline volcanics in northwestern Nigeria and a possible Pan-African suture zone: Earth and Planetary Science Letters, vol. 37: pp. 90–96.
Moreira, C.A. & Ilha, L.M. (2011). Prospecção, geofísica e ocorrência de cobre localizada na bacia sedimentar do Camaquã (RS). Revista da Escola de Minas, Ouro Preto, vol. **64** (3), pp. 309–315.
Moreira, C.A., Lopes, S.M., Schweig, C., Seixas, A.R. (2012). Geoelectrical prospection of disseminated sulfide mineral occurrences in Camaqua sedimentary basin, Rio Grande do Sul State, Brazil. Revista Brasileira de Geofísica, vol. **30** (2), pp. 169–179.

Mushayandebvu, M. F., Van Driel, P., Reid, A.B. & Fairhead, J.D. (2001). Magnetic source parameters of two-dimensional structures using extended Euler Deconvolution. Geophysics, vol. 66, pp. 814–823.

Muszala, S.P., N.R. Grindlay, & R.T. Bird (1999). Three-dimensional Euler Deconvolution and Tectonic Interpretation of Marine Magnetic Anomaly Data in the Puerto Rico Trench: Journal of Geophysical Research, vol. 29, pp. 175–187.

Nabighian, M. N. (1972). The Analytic Signal of two-dimensional magnetic bodies with polygonal cross-section: its properties and use for automated anomaly interpretation. Geophysics, vol. 37, pp. 507–517.

Nabighian, M. N. & Hansen, R. O. (2001). Unification of Euler and Werner Deconvolution in three dimensions via the generalized Hilbert transform. Geophysics, vol. 66, pp. 1805-1810.

Nwosu, E. I. (2018). Structural Interpretation of Part of Anambra Basin, Nigeria, using Aeromagnetic and Landsat ETM data. International Journal of Advances in Scientific Research and Engineering (IJASRE), vol. 4 (9), pp 49–59.

Obaje, N.G. (2009). Geology and mineral resources of Nigeria: Springer, Dordrecht, Heidelberg, London, and New York, pp. 221. http://dx.doi.org/10.1007/978-3-540-92685-6

Odeyemi, I. A. (1981). A review of the orogenic events in the Precambrian basement of Nigeria, West Africa. Geologische Rundschau, vol. 70: pp. 897–909.

Ogezi, A.E.O. (1977). Geochemistry and geochronology of basement rocks from northwestern Nigeria: Ph.D. dissertation, University of Leeds, England.

Okpoli, C. C. (2019). High-Resolution Magnetic Field Signatures Over Akure and Its Environs, Southwestern Nigeria. Earth Sciences Malaysia, vol. 3(1): pp. 09–17.

Oluyide, P.O. (1988). Structural trends in the Nigerian Basement Complex: Nigerian Mining Geology and Metallurgy Society, vol. 1, pp. 87–102.

Onyeagocha, A. C. & Ekwueme, B. N. (1982). The pre-Pan-African structural features of northcentral Nigeria". Journal of Mining and Geology, 19(2), pp. 74–77.

Osinowo, O. O. & Olayinka, A. I. (2013). Aeromagnetic Mapping of Basement Topography around the Ijebu-Ode Geological Transition Zone, Southwestern Nigeria: Acta Geodaetica et Geophysica, v. 48/3, pp. 451-470.

Oversby, V.M. (1975). Lead isotope study of aplites from the Precambrian rocks near Ibadan, Southwestern Nigeria. Earth Planetary Science Letters, vol. 27, pp. 177–180.

Rahaman, M. A. (1976). Review of the basement geology of Southwestern Nigeria, in Geology of Nigeria, edited by C.A. Kogbe: Elizabethan Publishers Company, Lagos, pp. 41–58.

Rahaman, M. A., Emofureta, W.O. & Caen Vachetta, M. (1983). The Potassic granites of the Igbetti area: further evidence of the polycyclic evolution of the Pan-African belt in Southwestern Nigeria. Precambrian Research. Vol. 22, pp. 25–92.

Rahaman, M. A. (1988). Recent Advances in the Study of the Basement Complex of Nigeria. Precambrian Research, vol. 38(1-3), pp. 83–100.

Raimi, J., Dewu, B.B.M. & Sule, P. (2014). An Interpretation of Structures from the Aeromagnetic Field over a Region in the Nigerian Younger Granite Province. International Journal of Geosciences, 5, 313–323. http://dx.doi.org/10.4236/ijg.2014.53031

Reeves, C.V., Reford, S.W. & Milligan, P. R. (1997). Airborne geophysics: Old methods, new images, Geophysics at the Millennium (A.G. Gubbins, editor), Proceedings of Exploration 97, 4th Decennial International Conference on Mineral Exploration, 14-18 September, Toronto, Ontario, pp. 13–30.

Reeves, C. V. (2005). Aeromagnetic Survey Principles, Practice and Interpretation. Geosoft, page 155.

Roy, L., Agarwal, B.N.P., and R.K. Shaw. (2000). A New Concept in Euler Deconvolution of Isolated Gravity Anomalies: Geophysical Prospecting, vol. 48(3), pp. 559–575.

Russ, W. (1957). The geology of parts of Niger, Zaria, and Sokoto provinces, with special reference to the occurrence of gold: Bulletin of Geological Survey Nigeria, page. 27.

Schetselaar, E. M. (2001). Petrogenetic interpretation from gamma-ray spectrometry and geological data: the Arch Lake zoned peraluminous granite intrusion. Western Canadian Shield. Exploration Geophysics, vol. **33**, pp. 35–43.

Thompson, D.T. (1982). EULDPH: A New Technique for Making Computer-Assisted Depth Estimates from Aeromagnetic Data, Geophysics, vol. 47: pp. 31-37

Turner, D.C. (1983). Upper Proterozoic schist belts in the Nigerian sector of the Pan-African province of West Africa: Precambrian Research, vol. 21: pp. 55–79.

Turner, D.C. & Webb, P.K. (1974). The Daura Igneous Complex, N. Nigeria: A link between the Younger Granite districts of Nigeria and S. Niger. Journ. Geol. Soc. Lond., 130, p. 71-77

Udo, R. K. (1978). Geographical Regions of Nigeria. Heinemann Educational Books

Van Breemen, O., Pidgeon, R.T. & Bowden, P. (1977). Age and isotopic studies of some panafrican granites from Northcentral Nigeria. Precambrian Research, vol. 4, pp. 307–319

White, C. E., Horne, R. J., Teniere, P. J., Jodrey, M. J., & King, M. S. (2001). Geology of the Meteghan River-Yarmouth area: a progress report on the Southwest Nova Scotia Mapping Project; in Minerals and Energy Branch, Report of Activities 2000; Nova Scotia Department of Natural Resources, Mines and Energy Branch, Report 2000-1, pp. 95–111.

Whitehead, N. & Musselman, C. (2008). MontajGravity/Magnetic Interpretation: Processing, Analysis and Visualization System for 3D Inversion of Potential Field Data for Oasis montaj v6.3, Geosoft Incorporated, 85 Richmond St. W., Toronto, Ontario, M5H 2C9, Canada.

Wright, J.B. (1976). Fracture systems in Nigeria and initiation of fracture zones in the South Atlantic. Tectonophysics, vol. 34: pp. 43–47.

Wright, J. B., Hastings, D. A., Jones, W. B., & Williams, H. R. (1985). Geology and mineral resources of West Africa. George Allen and Unwin, London, vol. 187, pp. 111–123.

Yin, L., John, S., Yingchang, C., Kongyou, W., Jian, W., Yannan, D., Yujie, L. & Zicheng, C. (2024). European Association of Geoscientists and Engineers; Basin Research, Volume 36, Issue 3. DOI: https://doi.org/10.1111/bre.12868